Phase Transformation of Stainless Steel During Fatigue

DANIEL HENNESSY, GARY STECKEL, AND CARL ALTSTETTER

Transformation of austenite during cyclic loading was studied in AISI 301 and 304 alloys whose stability was adjusted by heat treatment and temperature changes. Fatigue life was determined under controlled strain amplitude tension-compression conditions. The amount of transformation to α' (bcc) martensite was continuously indicated magnetically during testing, and the α' and ϵ (hcp) phases were observed metallographically at failure. It was found in room temperature testing that at strain amplitudes in excess of 0.4 pct the formation of α' (bcc) martensite was detrimental to the fatigue life. At 200°F (366 K) the fatigue life of an unstable alloy was increased, while in a completely stable austenitic alloy (20Cr, 6Ni, 9Mn), the life at 200°F (366 K) was less than that at room temperature for the same cyclic strain amplitude. The differing effect of temperature on life of these two types of alloy is attributed to the alteration of the austenite stacking fault energy and the relative free energies of the α' (bcc), ϵ (hcp) and γ (fcc) phases in the unstable alloys. It has been observed that within the standard composition ranges of the two 300 series stainless steel grades there can be marked differences in the degree of transformation resulting from cyclic loading. This has the implication that for fatigue applications modifications in the specifications for the different grades of stainless would be advantageous.

SEVERAL of the austenitic stainless steels are metastable at room temperature and undergo martensitic transformations as a form of plastic deformation. The formation of martensites increases the work hardening rate, resulting in high ultimate stress levels with good uniform elongation.[1] For monotonic tensile tests on stainless steels the stress-induced martensitic transformations have been described on macroscopic (Refs. 1 thru 5) and microscopic (Refs. 6 thru 9) levels. Only recently have investigators begin to explore the fatigue of unstable austenite, both in regard to crack propagation rates[10-12] and fatigue life.[13,14]

Though there is some controversy over the sequence of formation, it is well established that an hcp (ϵ) and a bcc (α') martensite may form either on cooling or upon stressing.I In general, as the solute content or the temperature increases the austenite becomes more stable. Breedis and Kaudman[15] have calculated relative free energies of the phases in the Fe-Cr-Ni system, and others have determined empirical relations for the M_S^{16} and M_D^2 temperatures. Not only the initiation of the transformation upon cooling or under stress is important, but also the course of transformation during straining will affect the mechanical behavior.[17] Furthermore, the localized transformation is important in determining mechanical behavior[13,18] and not merely the average amount at a given stress or strain. Nevertheless, for practical purposes it is helpful to quantify relationships between macroscopic measurements and fatigue behavior.

In low cycle fatigue it is frequently observed that when the total strain amplitude per cycle, $\Delta\epsilon$, is held constant, the fatigue life can be empirically related, and expressed simply, in terms of elastic strain amplitude, $\Delta\epsilon_e$, and the plastic strain amplitude, $\Delta\epsilon_p$, during a cycle.[19,20] A log-log plot of the cyclic total strain amplitude *vs* the number of stress reversals, $2N_f$,* in which failure is produced at that amplitude is a curve which can be analyzed into the sum of two straight lines. At high amplitudes the life is determined almost entirely by the amount of plastic deformation per cycle, whereas at low amplitudes there is very little macroscopic plastic deformation per cycle, and the elastic strain (or stress) is the controlling factor.

*Instead of the number of cycles to failure, N_f, the number of stress reversals, $2N_f$, is frequently used. In a monotonic test the material fails at one fourth cycle or one stress reversal.

Thus

$$\Delta\epsilon = \Delta\epsilon_e + \Delta\epsilon_p = \left(\frac{\sigma_f'}{E}\right)(2N_f)^{-b} + \epsilon_f'(2N_f)^{-c}$$

where E is the Young's modulus.

In many materials the empirical parameters σ_f' and ϵ_f' are the true fracture stress, σ_f and the true fracture ductility, ϵ_f respectively, as determined in a monotonic tensile test.[20] Sometimes the exponents b and c can be expressed simply in terms of the cyclic strain hardening exponent.[21]

The present experimental program examines the effect of phase transformation on fatigue life and conversely the effect of cyclic loading on the phase transformations. Tension-compression, total strain-controlled fatigue tests were made on three different austenitic stainless steels having different transformation behavior. The austenite stability of each steel was altered by testing at elevated temperatures approaching the M_D temperature and by using different annealing treatments to control austenite composition. A magnetic technique was used during cycling to monitor the formation of α' martensite, while light and

DANIEL HENNESSY, formerly a Research Assistant, is now with Essex International, Ft. Wayne, IN. GARY STECKEL is presently a Research Assistant at the University of Illinois. CARL ALTSTETTER is a member of the Metallurgy Department and the Materials Research Laboratory of the University of Illinois at Urbana-Champaign, IL 61801.

Manuscript submitted June 29, 1975.

electron microscopy yielded further information about the transformation products and fracture characteristics.

EXPERIMENTAL PROCEDURE

Commercial heats of AISI type 301 and type 304 austenitic stainless steels and Armco 21-6-9* were studied. The 300-series alloys were selected because they are among the most unstable, that is, the most susceptible to martensite formation, of the austenitic stainless steels. The 21-6-9 alloy was chosen because of its stability. The chemical composition of each material is given in Table I. The 301 and 304 specimens had a uniform diameter section 0.30 in. (7.62 mm) long with a diameter of 0.13 in. (3.30 mm), while the 21-6-9 specimens had a 0.25 in. (6.35 mm) diam. They were annealed in a vacuum of less than 10^{-5} Torr (0.13 Pa) for 30 min, either at 2000°F (1366 K) or 1750°F (1227 K). Those specimens annealed at the higher temperature were oil quenched, while the others were furnace cooled [3 h from 1750°F (1227 K) to less than 400°F (477 K)]. In the slowly cooled specimens, precipitation of chromium carbide reduced the carbon and chromium concentration in the austenite, rendering it more unstable than in the oil quenched condition. No martensitic product was observed magnetically or microscopically at room temperature, even in specimens which had been cooled to 77 K prior to measurement. After heat treatment all samples were electropolished and then heated at 392°F (473 K) to remove hydrogen. Monotonic tensile properties of the AISI steels in these conditions are given in Table II.

*This material, now known as Nitronic 40, was donated by the Armco Steel Corporation.

Table I. Chemical Composition of Alloys, Wt Pct

Element	301	304	21-6-9
C	0.107	0.062	0.007
Cr	17.31	18.30	20.04
Ni	7.37	8.64	6.67
Mn	1.90	0.55	8.73
P	0.035	0.022	0.017
S	0.024	0.015	0.016
Si	0.42	0.47	0.19
Mo	0.48	0.10	—
Cu	0.28	0.06	—
N	—	—	0.31
Ti	—	—	0.014
Fe	Balance	Balance	Balance

Fatigue tests were performed in air at room temperature, 200°F (366 K) and 240°F (389 K) using an MTS electrohydraulic closed-loop system. A fusible metal gripping arrangement was used to insure good alignment, no grip back-lash, and minimal clamping stresses.[22] Specimens were first threaded into the load cell and then into a steel plug around which the fusible alloy was allowed to solidify. Longitudinal strain over a 0.2 in. (5.1 mm) gage length was measured with a clip-on extensometer and controlled at various levels from ± 0.3 pct to ± 3.0 pct. Tests were conducted using a triangular wave form and cyclic frequencies between 0.1 and 1.0 Hz (strain rate of the order of 0.5/min). For the elevated temperature tests a small furnace surrounded the specimen and extensometer. At various times during the life of the specimen the stress-strain hysteresis loop was plotted.

A measure of the amount of BCC martensite was obtained using a commercial "ferrite detector" sensitive to changes in magnetic permeability. Lineal analysis of metallographic specimens taken after cyclic loading and measurements on compacted powder mixtures of known composition were used to calibrate the instrument in terms of the absolute quantity of magnetic phase under no-load conditions. The output voltage of the ferrite detector could be readily standardized using a known specimen and was very reproducible and stable. Relative changes corresponding to a fraction of a volume percent could be easily recorded. The transducer was mounted within the gage length of the specimen and its output was recorded as a function of stress or strain during cycling.

After fatigue failure the fracture surfaces were examined with a scanning electron microscope. Speci-

Table II. Monotonic Tensile Properties, Annealed 1750°F (1227 K), Furnace Cooled (Data in parentheses are for material oil quenched from 2000°F (1366 K)

	Type 301			Type 304		
Test temperature, °F (K)	72°F (295 K)	200°F (366 K)	240°F (389 K)	72°F (295 K)	200°F (366 K)	240°F (389 K)
0.2 Pct offset yeild strength (MPa)	(262) 276	255	234	(241) 262	221	214
True fracture strength, σ_f (MPa)	(2144) 2199	2213	2192	(2165) 2386	1800	1910
Reduction in area, pct	(68) 67	75	71	(79) 69	84	79
True fracture ductility, ϵ_f	(1.15) 1.10	1.39	1.24	(1.55) 1.12	1.85	1.55
Strain hardening exponent (approximate)	0.07	0.07	0.07	0.11	0.07	0.06
Magnetic phase at fracture, pct	50	2.7	1.5	65	3.9	1.4
Rockwell B. hardness	(78) 80			(75) 80		

mens from the gage length were also prepared for optical and transmission electron microscopy. Sectioning was done with a slow speed diamond saw, and after careful grinding the specimens were electropolished to remove all traces of transformation during preparation of the surfaces or foils. Electropolishing and thinning were done using a twenty parts glacial acetic acid, ten parts perchloric acid, one part water electrolyte at 8 volts. Electroetching was done in a 10 pct oxalic acid solution at 8 volts.

RESULTS

Mechanical Testing

Fig. 1 for type 301 steel is representative of the strain-life data for all materials tested. The total strain was analyzed into the plastic strain amplitude, $\Delta\epsilon_p$, which is half the width of the hysteresis loop at zero stress, and the elastic strain amplitude, $\Delta\epsilon_e$, which is the maximum stress divided by Young's modulus. For all the materials and temperatures the logarithm of these strain amplitudes varied linearly with the logarithm of the number of reversals to cause failure. The parameters in Eq. [1], which thus succinctly describes the data, are given in Table III. They were obtained by a least squares fit of the data points.

Typical plots of stress *vs* strain are shown for ± 1.5 pct and ± 0.5 pct cyclic strain in the lower part of Fig. 2 and 3, respectively, at various times throughout the life of type 301 steel specimens. Generally, all the materials cyclically hardened throughout their life except at low strain amplitudes ($\gtrsim$ 0.5 pct), where slight softening occurred. In Figs. 2 and 3 the change in magnetic response is also shown as a function of strain. At the left-hand side of Fig. 2 the output of the detector is recorded starting from the initiation of the test. As the load increased in the first half-cycle, so also did the indicated amount of transformation. This is in accord with expectations. After several loading cycles a hysteresis loop developed. These hysteresis loops are shown in Figs. 2 and 3 with the origin of the plots superimposed on the origin of the stress-strain loops, denoted by a cross. It will be shown later that as the stress or strain changes two factors may contribute to the indicated permeability change: 1) change in permeability of existing ferromagnetic phase (magnetomechanical effect) and 2) change in percent of ferromagnetic phase. The center of the hysteresis loop (average value of ordinate at zero strain) was taken as an indication of the amount of transformation which occurred, because this approximates the conditions under which the device was calibrated. It may be seen that the indicated value at the center of the hysteresis loops increased with the number of loading cycles. This trend throughout the life of the specimen is shown in Fig. 4 for a strain amplitude of 1.5 pct for the 301 and 304 steels tested at the three temperatures. Two trends may be noted from this plot: first, under fatigue conditions this particular heat of 301 steel transformed less extensively than the 304 material at room temperature; second, an increase of testing temperature by roughly 100 K caused a sharp decrease in the amount of bcc martensite formed. This suggests that the M_D for cyclic loading is somewhat above 240°F (389 K).

Further characterization of the transformation behavior is presented in Fig. 5, where it can be seen that the amount of martensite at fracture is a function of the strain amplitude. It is important to note here that the magnetic measurement was made on the lateral surface of the test section adjacent to the fracture surface, and it does not give exactly the amount of phase at the fatigue crack. Generally, however, the reading was higher near the fracture than away from it, indicating that transformation was enhanced in the plastic zone at the crack tip. Unfortunately, comparable measurements of the amount of HCP phase were not obtained during cycling.

Metallography

In the undeformed condition there was no metallographic evidence of martensitic transformation of the austenite. In the slowly cooled 301 and 304 alloys car-

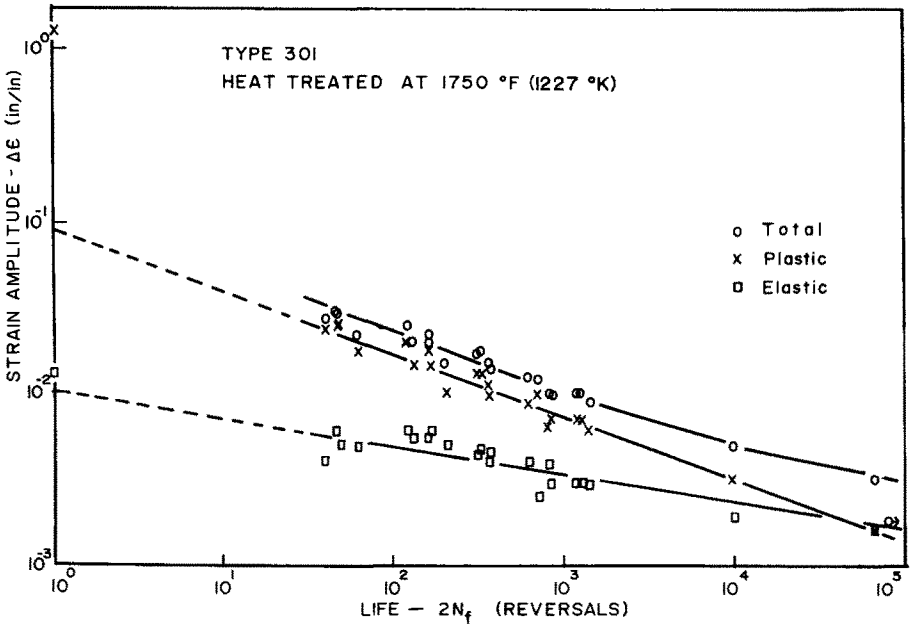

Fig. 1—Strain-life relations for type 301 stainless steel tested at 72°F (295 K).

Table III. Fatigue Parameters Annealed 1750°F (1227 K), Furnace Cooled
(Data in parentheses are for material oil quenced from 2000°F (1366 K)

$$\Delta\epsilon = \frac{\sigma_f'}{E}(2N_f)^{-b} + \epsilon_f'(2N_f)^{-c}$$

Test temperature °F (K)	Type 21-6-9 (295 K)	Type 301 (205 K)	Type 301 (366 K)	Type 301 (389 K	Type 304 (295 K)	Type 304 (366 K)	Type 304 (389 K)
Ductility exponent, c	0.415	(0.378) 0.359	0.459	0.453	(0.267) 0.314	0.398	0.384
Ductility coefficient, ϵ_f'	0.376	(0.115) 0.088	0.282	0.267	(0.036) 0.047	0.189	0.165
Strength exponent, b	0.229	(0.245) 0.158	0.205	0.214	(0.088) 0.090	0.213	0.153
Strength coefficient ÷ Young's modulus, σ_f'/E	0.018	(0.015) 0.010	0.013	0.012	(0.006) 0.006	0.013	0.007
Approximate volume pct magnetic phase at fracture for ±1 pct strain	0	(8) 30	6	3	(40) 55	8	4

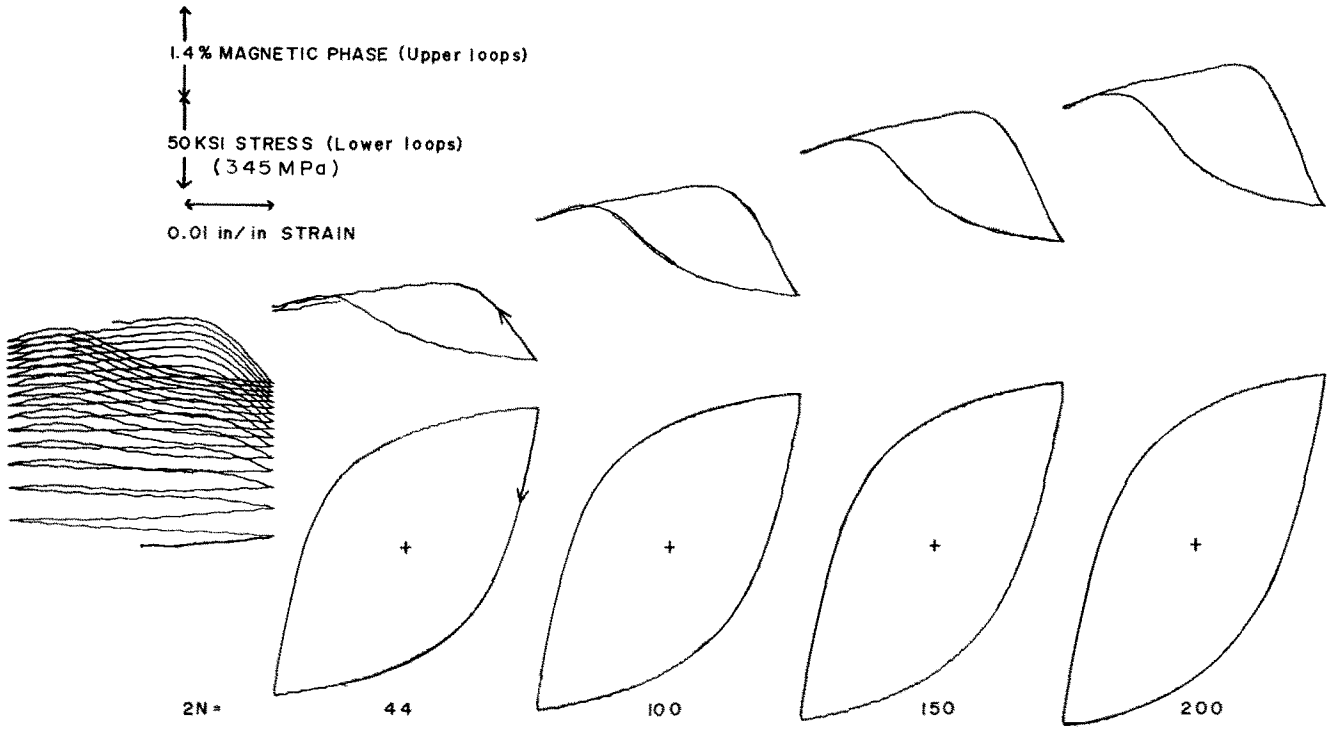

Fig. 2—Change in hysteresis with number of reversals ($2N$) for type 301 stainless steel furnace cooled from 1750°F (1227 K) and tested at 72°F (295 K). Cycled at $\Delta\epsilon = \pm 1.5$ pct, $2N_f = 358$. Lower portion—stress *vs* strain Upper portion—magnetic phase *vs* strain. The cross designates the origin of both sets of hysteresis loops.

bide precipitation made the grain boundaries etch deeply and caused much pitting within the grain interior, in contrast to the oil quenched material and the 21-6-9 alloy, in which carbide precipitation was not observed or expected. No martensitic transformation product was observed under any condition in the 21-6-9 alloy. Fig. 6 for type 304 steel serves to illustrate the form and distribution of martensitic phases resulting from cyclic loading of types 301 and 304 steels. The HCP phase appeared as thin parallel individual striations or packets, occasionally extending completely across grains. When present on more than one habit plane these platelets did not interpenetrate, a feature which distinguished them from slip lines; however, the possibility that some of these platelets were deformation twins could not be discounted. The frequent parallelism with annealing twin traces was consistent with their expected {111} habit. The distribution of these plates was highly inhomogeneous, with dense packets in some grains and none in others. There was also occasionally a nonuniformity across the specimen cross section, suggesting chemical or stress (strain) inhomogeneity. The α' phase appeared in two microstructurally distinguishable forms. In the

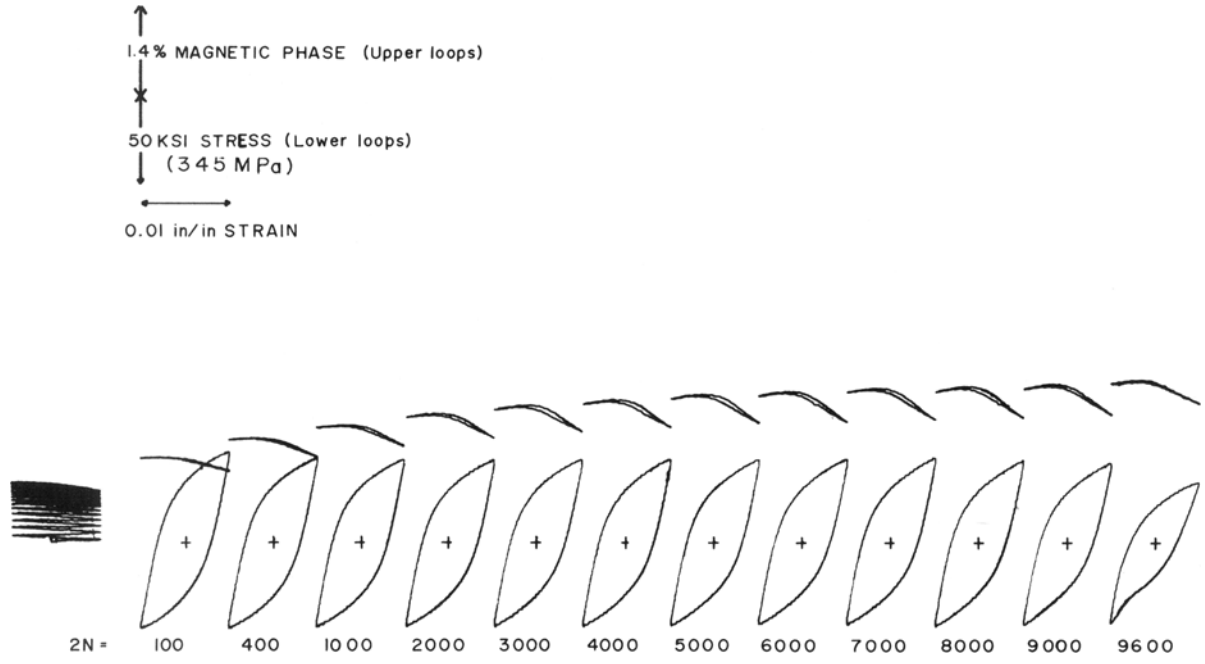

Fig. 3—Change in hysteresis with number of reversals ($2N$) for type 301 stainless steel furnace cooled from 1750°F (1227 K) and tested at 72°F (295 K). Cycled at $\Delta\epsilon = \pm 0.5$ pct, $2N_f = 9870$. Lower portion—stress *vs* strain. Upper portion—magnetic phase *vs* strain. The cross designates the origin of both sets of hysteresis loops.

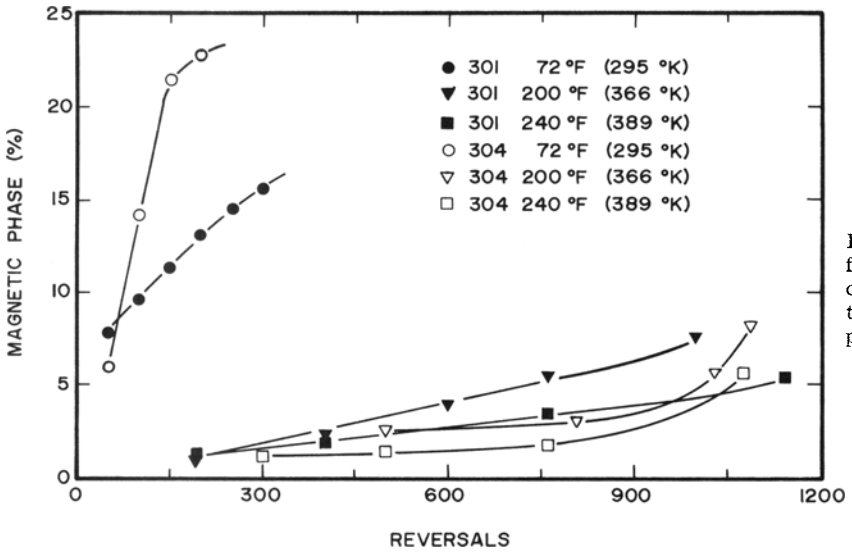

Fig. 4—Magnetic phase *vs* number of reversals for type 301 and 304 stainless steel furnace cooled from 1750°C (1227 K) and tested at the temperatures indicated. Cycled at $\Delta\epsilon = \pm 1.5$ pct.

absence of observable hcp phase the α' had an elongated blocky shape as at A in Fig. 6. When ϵ phase was present, the BCC phase was also formed along the ϵ platelets giving it a more feathery or lathlike appearance as at B in Fig. 6. Slip lines, and particularly their intersections, were also favored sites from which the α' laths grew.

The optical metallographic results confirmed the indications of the magnetic detection method for the α' martensite, Figs. 4 and 5 and Table II, for the effect of austenite stability. That is, at elevated test temperature or low strain amplitudes less transformation was observed. Also, in the quenched specimens, the austenite was more stable than in the furnace cooled ones. It was difficult to be precise about the relative amounts of α' and ϵ phases as the austenite composition, test temperature, strain amplitude and number of cycles was varied. This was largely due to the intermixture of the phases, the inhomogeneous distribution and the difficulty in estimating volume of thin platelets. Generally, it appeared that the lower the strain amplitude or higher the test temperature, the less ϵ phase was present. Thus, for example, at ± 0.5 pct strain amplitude at 240°F (389 K) the α had the blocky form. At higher strain amplitudes and lower test temperatures there was little of the blocky form of α', and the austenite was replaced by the feathery mixture of α' and ϵ. The 301 and 304 alloys differed only in the amounts of the phases present, not in their morphology. At fracture this particular heat of 304 stainless tended to have roughly 50 pct more transformation to both martensitic phases then the

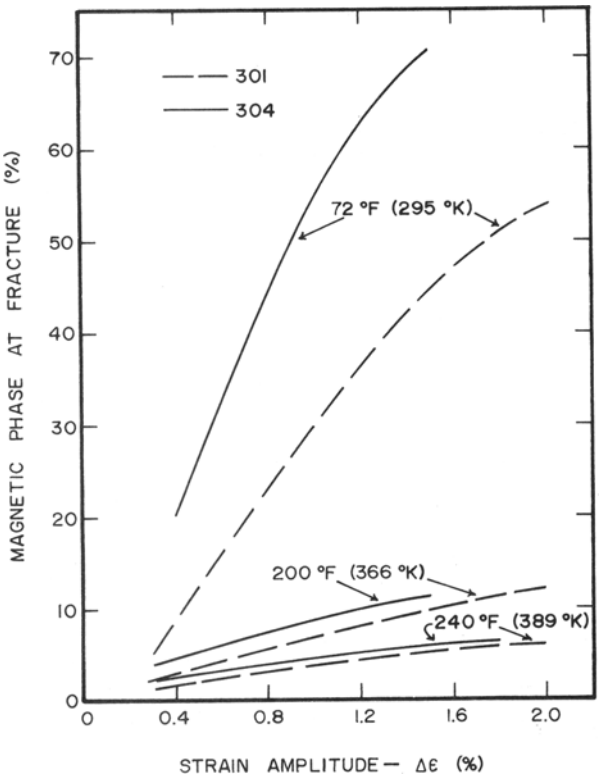

Fig. 5—Magnetic phase at fracture v_S strain amplitude for type 301 and 304 stainless steel furnace cooled from 1750°F (1227 K) and tested at the temperatures indicated.

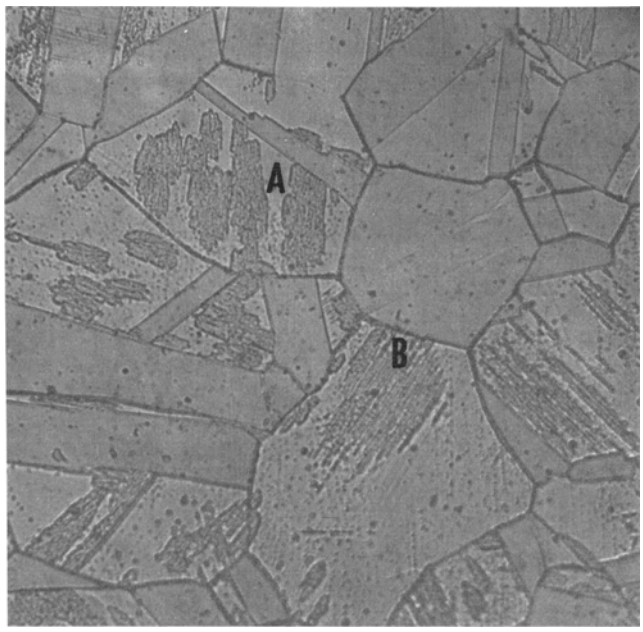

Fig. 6—Light micrograph of type 304 stainless steel furnace cooled from 1750°F (1227 K) and tested at 200°F (366 K). Cycled at $\Delta\epsilon$ = 1.5 pct, $2N_f$ = 1031. Magnification 388 times. **A** and **B** denote different morphologies of α' martensite.

301 type under identical conditions of strain amplitude and test temperature, in agreement with Fig. 5.

Transmission electron micrographs in the annealed, undeformed condition showed no hcp or bcc martensite. In furnace cooled specimens carbide particles averaging 0.3 μm in diam were observed at grain boundaries, but there were none in the oil quenched specimens. In specimens of 301 deformed once to 1 pct strain at room temperature a high density of stacking faults and dislocations was observed, but there were no transformation products. In the same alloy cycled to failure at ± 1.5 pct strain amplitude (662 cycles) and room temperature, bands of ϵ were present with α' associated with them. It was difficult to clearly image and get sharp diffraction patterns from these specimens due to the high density of dislocations, stacking faults and transformation product. Yet in some areas only austenite was observed and in other areas only ferrite was observed. The latter areas were very probably the blocky α'. When not in contact with ϵ, some isolated α' particles had a lenticular form. Fig. 7 illustrates the relationship between the ϵ and lath α' constituents. Dark field imaging using hcp and bcc reflections confirmed that the α' was growing at and apparently replacing the ϵ bands. After fatigue deformation there was evidence of cell formation in the austenite but no observable extension of partial dislocations in the cell walls.

Fracture surfaces were examined in the scanning electron microscope after fatigue failure at room temperature. In the unstable alloys the fracture was partly intergranular, Fig. 8, regardless of heat treatment. In nearly all specimens the region of fatigue crack initiation and advance had a flat, brittle appearance (quasi-

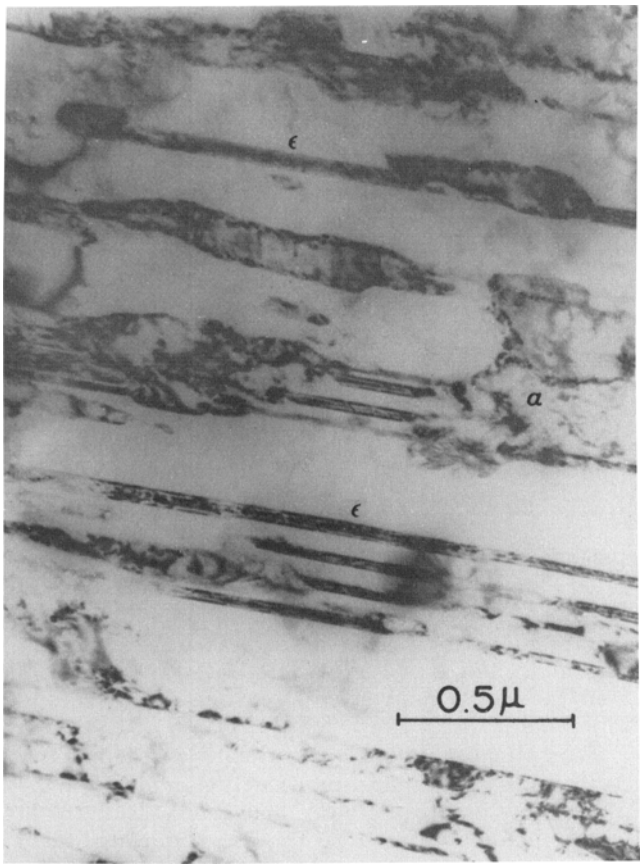

Fig. 7—Transmission electron micrograph of type 301 stainless steel oil quenched from 2000°F (1366 K) and tested at 72°F (295 K). Cycled at $\Delta\epsilon$ = ± 1.5 pct, $2N_f$ = 662. Plane of foil is $(112)\gamma \parallel (120)\alpha'$.

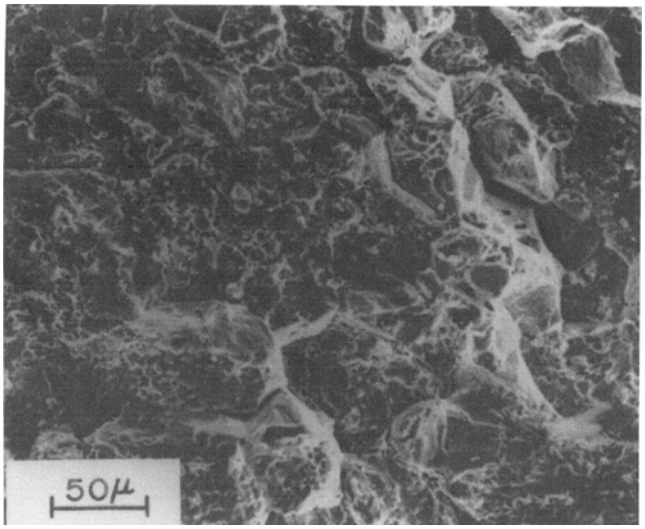

Fig. 8—Scanning electron micrograph of type 301 stainless steel furnace cooled from 1750°F (1227 K) and tested at 72°F (295 K). Cycled at $\Delta\epsilon = \pm 1.0$ pct, $2N_f = 1193$.

cleavage). In specimens tested at 0.5 pct or lower strain amplitudes fatigue striations were often present in this region. The region of fast, overload fracture had a typical dimpled or microvoid coalescence appearance.

DISCUSSION

Fatigue Life

Several of the parameters used to describe fatigue life, Table III, are anomalous in comparison with the normal ranges obtained from stable engineering materials. The fatigue ductility exponent, c, tends to be considerably less than one-half, as originally given in the Coffin-Manson relation, or the range from 0.5 to 0.7 found for a variety of materials.[23] In this work, if the materials are ranked in order of increasing stability by noting the amount of α', formed at failure under ± 1 pct strain amplitude, one has 304 (295 K), 301 (295 K), 304 (366 K), 301 (366 K). In this same order the fatigue ductility parameter was found to increase monotonically from ~0.30 to ~0.35 to ~0.40 to ~0.45. Thus, the indication here is that unstable material would have a greater amount of plastic strain at long life than the stable material, other things being equal. Fig. 9, comparing 301 stainless with several types of stable materials, also demonstrates this trend. Unfortunately when one compares values for the fatigue ductility coefficient, ϵ_f' (Table III) with the true fracture ductility, ϵ_f (Table II), one observes that this parameter is a factor of five to ten lower in fatigue. Stated another way, the plastic strain *vs* life curves for the 300 series steels tested have relatively small intercepts compared to stable materials, for which the true fracture ductility in a monotonic tensile test can be used to roughly predict fatigue behavior, according to the Coffin-Manson law. In contrast, Chanani and Antolovich found that the Coffin-Manson law was indeed obeyed for TRIP steels, which transformed during fatigue.[13] The parameter b for the present materials varied from roughly 0.09 to 0.25, somewhat above values for stable materials, which range from 0.05 to 0.15.[20] Values of the fatigue strength co-efficient, σ_f', were generally somewhat above the true fracture strength, σ_f just as in the case for many other materials.[20]

Figs. 10 and 11 summarize the effect of temperature, and therefore austenite stability, on the fatigue life of type 301 and 304 steels, respectively. From both these plots it seems clear that above a strain amplitude of about 0.5 pct, martensitic transformation of austenite can decrease fatigue life by as much as a factor of three or four, whereas below 0.5 pct some martensite formation may be beneficial. It must be appreciated, of course, that the amount of transformation is dependent not only on the temperature of testing, but also on the strain amplitude, so that the amount of martensite varies along each curve. The situation is even more complicated in that the macroscopic measurements (strain, stress, magnetization) used to characterize the tests do not reflect the local conditions at the crack tip. Unfortunately, metallographic techniques for observing martensitic formation at the crack tip cannot be conveniently adapted for use under cyclic conditions. Nevertheless, it is an important result of this study to indicate that martensitic transformation can be an influential factor in determining fatigue behavior, either improving or degrading the life. This suggests that for fatigue applications the designer must take into account the temperatures, temperature cycling, and cyclic strain or stress range in order to optimize performance. Some guide to the metastability of the steel in fatigue is provided by the amount of α' at fracture in a monotonic tensile test; compare Tables II and III. It is proposed that 1 to 4 pct α' formed in the tensile test may indicate a desirable instability for low strain fatigue.

Fig. 12 compares fatigue lives of the three steels at room temperature. The 21-6-9 alloy is obviously superior to the AISI alloys at high strain amplitudes. Whether this advantage is due solely to its nontransformability is uncertain, since its composition is rather different from the others. At any rate there are indications that the more unstable 304 composition may be superior to the 21-6-9 at low strains. Moreover, the effect of increasing the temperature was to move the 301 and 304 curves to longer lives, whereas a few tests in the 21-6-9 alloy at elevated temperatures gave shorter fatigue lives.

The deleterious effect of large amounts of α' formation on fatigue life at high strain amplitude is in agreement with the conclusion of Chanani and Antolovich for TRIP steel.[13] Yet this finding must be reconciled with the fact that in TRIP steels[10] and unstable austenitic stainless steels[11,12] fatigue crack growth rate in notched specimens is lowered as the steel is made more unstable. This apparent contradiction in the effect of martensite formation may be found also in the cross-over of the curves in Figs. 10, 11, and 12. It is proposed that the explanation lies in the difference between crack propagation in an α'/γ matrix and that in an austenitic matrix which transforms at the crack tip. The former is the case of our tests at high strain amplitude; the latter is more characteristic of our tests at low strain amplitudes. It is not nec-

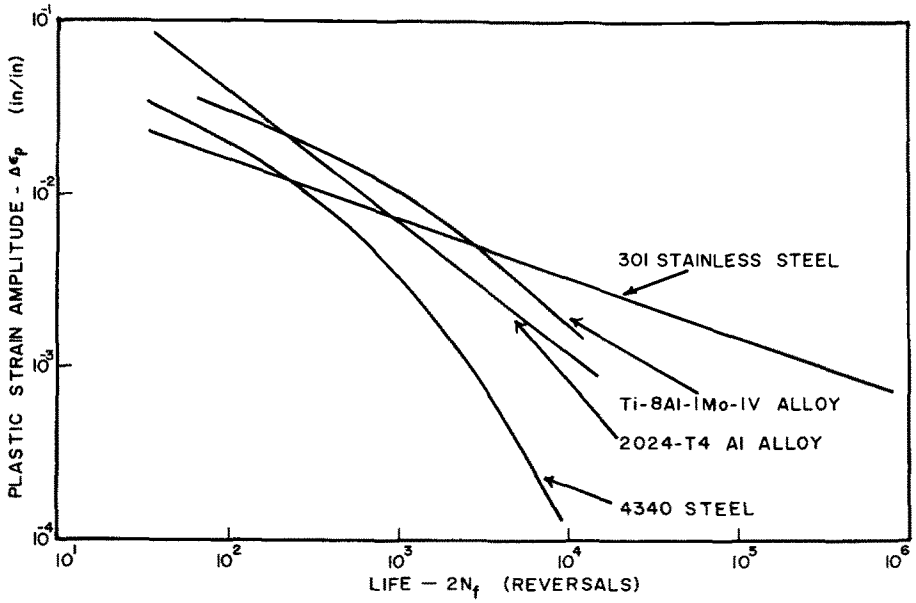

Fig. 9—Comparison of plastic strain-life relations for type 301 stainless steel and other engineering materials tested at room temperature.

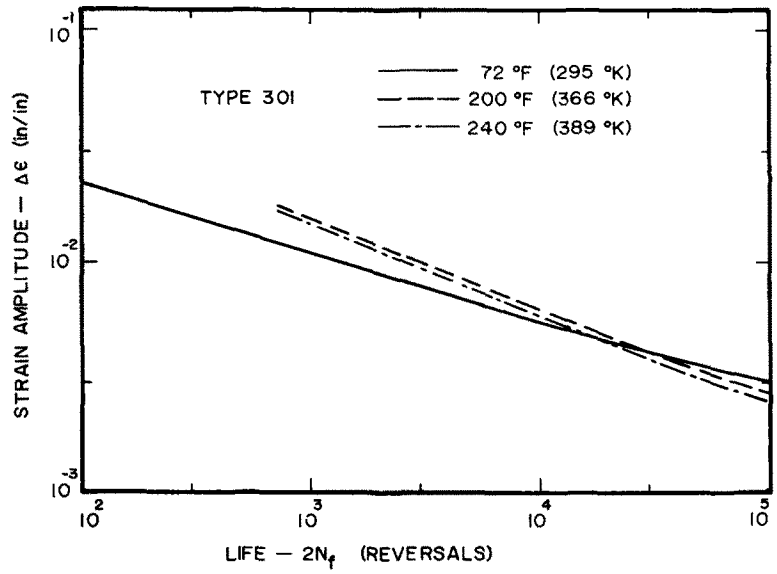

Fig. 10—Comparison of strain-life relations for type 301 stainless steel furnace cooled from 1750°F (1227 K) and tested at the temperatures indicated.

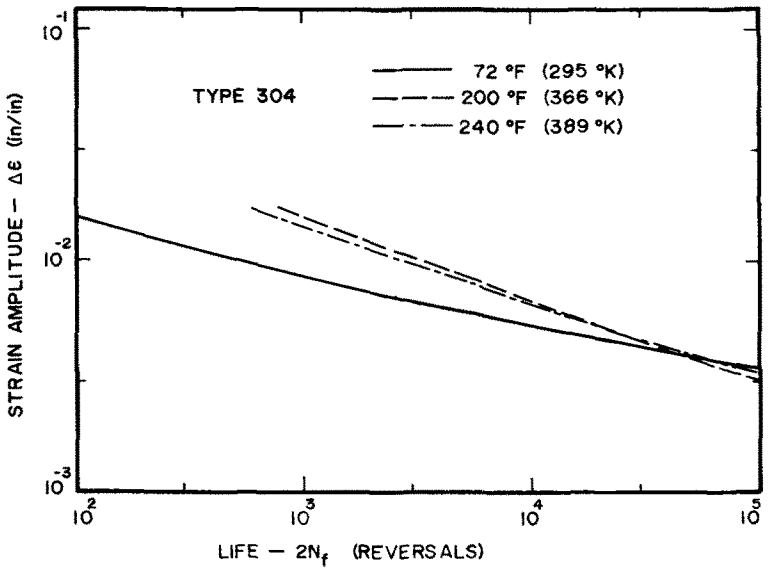

Fig. 11—Comparison of strain-life relations for type 304 stainless steel furnace cooled from 1750°F (1227 K) and tested at the temperatures indicated.

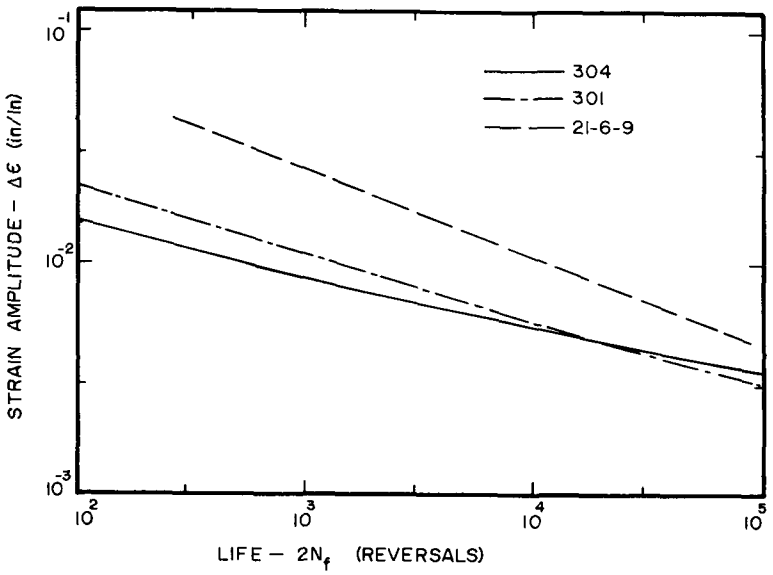

Fig. 12—Comparison of strain-life relations for type 301, 304, and 21-6-9 stainless steel furnace cooled from 1750°F (1227 K) and tested at 72°F (295 K).

essary to reiterate the arguments of why crack tip plasticity should be beneficial.[11] In the prenotched specimens used in crack growth studies there is not a great amount of transformation throughout the specimen as there is in smooth fatigue specimens at high strain amplitudes. Instead, the transformation is more localized to the crack tip, where it probably does the most good in relieving the stress concentration and creating favorable residual stress in the plastic zone.[12,24] This latter effect of transformation-induced plasticity is enhanced due to the fact that the γ-α' transformation results in a volume increase, and thus residual compressive stress. Further evidence of this is found in our result that there is a tendency to develop a mean compressive stress in controlled strain amplitude tests in which a large amount of α' is formed.

Stress-induced reversal of transformation to and from the magnetic α' phase has not been reported in the literature for these alloys. Because of the transformation shear strain the reversal of transformation under load could contribute an important means of plastic accommodation at the crack tip. It is a possible source of the observed large plastic strain component observed at low total strain amplitudes, Fig. 9, just where the unstable material has longer life than more stable material. Without further information it is difficult to interpret the details of the magnetic hysteresis curves such as those in Figs. 2 and 3. To help in the task of separating stress-induced transformation from magnetomechanical effects normalized low carbon steel and quenched and tempered alloy steel were cyclically stressed. The measured changes in magnetic detector output were normalized by dividing by the average output. These normalized plots, Fig. 13, indicate that in the stainless steels the volume fraction of α' may well be changing, because the fractional change in magnetic output is far greater than in the steels which cannot undergo stress-induced transformation, yet would be expected to show appreciable magnetomechanical effects. Reversibility of the transformation strain could represent a less damaging plastic deformation mode than slip. Since the $\gamma \rightleftarrows \alpha'$ transformation mechanism is not known, however, it is difficult to further amplify this suggestion. It has been previously demonstrated, however, that reversible twin boundary motion will allow ferroelastic materials to undergo millions of cycles at ± 5 pct strain.[25]

Another possible benefit of the relatively large plastic strain in the unstable alloys is the resultant mechanical energy dissipation, as given by the area of the hysteresis loops. Under the controlled strain tests of this investigation this benefit would not be as apparent as in a resonating component. It has long been recognized that in some applications austenitic alloys are at a disadvantage compared with ferritic alloys, which dissipate vibrational mechanical energy through magnetomechanical damping.[26] Transformation hysteresis could be an alternate mechanism for damping in unstable "austenitic" alloys.

Transformation Behavior

The present metallographic results indicate that α' can form from either the γ or ϵ phases, and its morphology depends on which phase is the parent phase. This finding for transformation under fatigue conditions is in agreement with that for monotonic stress-induced transformation. Two α' morphologies were seen by Lecroisey and Pineau[9] and also by Lagneborg[7] and Goodchild *et al*,[27] who observed that crystallographic orientation with respect to the stress axis was important in determining whether α' formed with or without the ϵ phase. Langenborg's model rationalizes the nucleation of α' at ϵ phase but does not explain the growth, nor the blocky α' formed in the absence of ϵ. We note disagreement with Mangonon and Thomas[3] and others,[28] who have concluded that α' forms only when ϵ is present. Yet another school of thought has ϵ forming because of prior α' formation.[29] It is likely that all of these conclusions, though seemingly contradictory, are correct. As Breedis[30] and others[9] have demonstrated, the morphology is a sensitive function of composition. This factor, along with the temperature, determines the relative free energies of the three phases, and also the stacking fault energy of the austenite. This latter factor determines its deformation behavior and influences the nucleation and the morphology of the margensitic phases. Discrepancies between investigators thus may be attributable

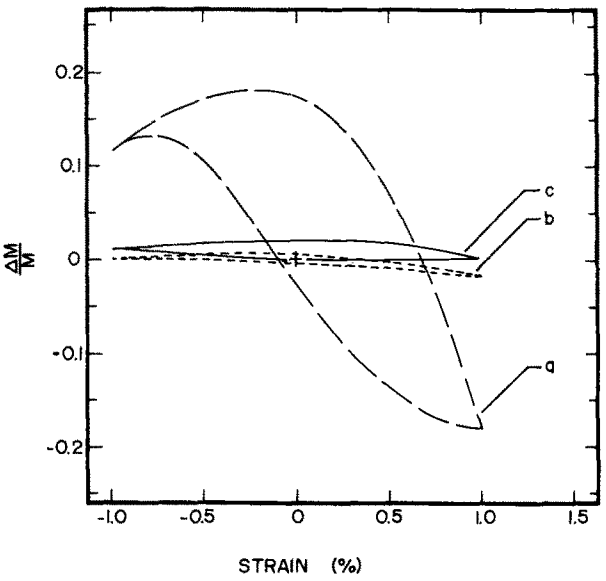

Fig. 13—Examples of fractional change in magnetic response ($\Delta M/M$) *vs* strain hysteresis. Cycled at $\Delta\epsilon = \pm 1.0$ pct at 72°F (295 K). (*a*) Type 301 stainless steel furnace cooled from 1750°F (1227 K). (*b*) Oil quenched and tempered (600°F (590 K for 1 h) AISI 4340 steel. (*c*) Normalized mild steel.

to slight differences in composition of nominally identical alloys. It should be noted here that the AISI composition limits for stainless steels are too broad to adequately characterize transformation behavior. For example, the 301 steel used in this study formed less α' than the 304 steel, yet it is widely believed that AISI 301 is less stable than AISI 304. This confusion is further compounded by unintentional matrix compositional changes due to different heat treatments or application temperatures which allow precipitation of carbides. Carburization and decarburization in service can also significantly change the transformability. Hydrogen produced by aqueous corrosion or from gaseous environments is said to lower the FCC stacking fault energy,[31] leading to changes in transformation characteristics throughout the service life of a component.

The amount of martensite increases progressively during the fatigue life, Fig. 4, so that for a given strain the amount of α' can be related to the number of cycles. The ease of detection of α' by magnetic means suggests that nondestructive evaluation of fatigue damage could be conveniently done magnetically. Components could be removed from service and scanned magnetically in order to reveal general or localized damage. It is not unreasonable to expect that the technique might be developed to reveal potential failure locations even before cracks have formed. In fact, an NDE advantage could constitute a sufficient reason for designing with material of known instability.

CONCLUSION

We have shown in this work that the degree of instability of austenite is an important factor in determining its fatigue behavior, either improving or degrading it, depending on the amount of martensite formed and the cyclic strain amplitude. Because of the effect of steel composition and service conditions on the transformation, design of stainless steel components which are cyclically stressed must be carefully optimized. This is of particular importance for subambient temperatures, which favor transformation. Material for critical components should be individually characterized with regard to transformation behavior, since the commercially specified alloy designations have composition ranges which are too broad for this purpose.

ACKNOWLEDGMENT

This research was supported by the U. S. Army Research Office (Durham) under grant 31-124-G1149. The use of facilities of the Materials Research Laboratory is acknowledged. The authors especially wish to thank Professor Jodean Morrow of the Theoretical and Applied Mechanics Department for his helpful suggestions and continued interest in this work.

REFERENCES

1. J. P. Bressanelli and A. Moskowitz: *Trans. ASM*, 1966, vol. 59, pp. 223-39.
2. T. Angel: *J. Iron Steel Inst.*, 1954, vol. 177, pp. 165-72.
3. C. Guntner and R. Reed: *Trans. ASM*, 1962, vol. 55, pp. 399-419.
4. D. Neff, T. Mitchell and A. Troiano: *Trans. ASM*, 1969, vol. 62, pp. 858-62.
5. G. Stone and G. Thomas: *Met. Trans.*, 1974, vol. 5, pp. 2095-102.
6. B. Cina: *Acta Met.*, 1958, vol. 6, pp. 748-62.
7. R. Lagneborg: *Acta Met.*, 1964, vol. 12, pp. 823-43.
8. P. Mangonon and G. Thomas: *Met. Trans.*, 1970, vol. 1, pp. 1577-86.
9. F. Lecroisey and A. Pineau: *Met. Trans.*, 1972, vol. 3, pp. 387-96.
10. G. Chanani, S. Antolovich, and W. Gerberich: *Met. Trans.*, 1972, vol. 3, pp. 2661-72.
11. C. Bathias and R. Pelloux: *Met. Trans.*, 1973, vol. 4, pp. 1265-73.
12. A. Pineau and R. Pelloux: *Met. Trans.*, 1974, vol. 5, pp. 1103-12.
13. G. Chanani and S. Antolovich: *Met. Trans.*, 1974, vol. 5, pp. 217-29.
14. C. Altstetter and D. Hennessy: *The Microstructure and Design of Alloys*, pp. 437-40, Institute of Metals, London, 1974.
15. J. Breedis and L. Kaufman: *Met. Trans.*, 1971, vol. 2, pp. 2359-71.
16. G. Eichelman and F. Hull: *Trans. ASM*, 1953, vol. 45, pp. 77-104.
17. D. Brandarkar, V. Zackay, and E. Parker: *Met. Trans.*, 1972, vol. 3, pp. 2619-31.
18. A. Rosen, R. Jago, and T. Kjer: *J. Mater. Sci.*, 1972, vol. 7, pp. 870-76.
19. R. Smith, M. Hirschberg, and S. Manson: NASA technical note D1574, 1963.
20. R. Landgraf: ASTM, STP 467, pp. 3-36, 1970.
21. J. Morrow: ASTM, STP 378, pp. 45-87, 1965.
22. C. Feltner and M. Mitchell: ASTM, STP 465, pp. 27-66, 1970.
23. L. Coffin: *Ann. Rev. Mater. Sci.*, 1972, vol. 2, pp. 313-48.
24. C. Bathias and R. Pelloux (discussion of Ref. 12): *Met. Trans.*, 1974, vol. 5, pp. 306-07.
25. R. Karz: Ph.D. dissertation, 1972, University of Illinois, Urbana, Il.
26. A. Cochardt: *Magnetic Properties of Metals and Alloys*, pp. 251-79, ASM, Metals Park, Ohio, 1959.
27. D. Goodchild, W. Roberts, and D. Wilson: *Acta Met.*, 1970, vol. 18, pp. 1137-45.
28. J. Breedis and W. Robertson: *Acta Met.*, 1962, vol. 10, pp. 1077-88.
29. J. Dash and H. Otte: *Acta Met.*, 1963, vol. 11, pp. 1169-78.
30. J. Breedis: *Trans. TMS-AIME*, 1964, vol. 230, pp. 1583-96.
31. M. Holzworth and M. Louthan: *Corrosion*, 1968, vol. 24, pp. 110-24.